

Steady-state phases in long-range measurement-only quantum circuits

Bihui Zhu

*Homer L. Dodge Department of Physics and Astronomy,
The University of Oklahoma, Norman, Oklahoma 73019, USA*

*Center for Quantum Research and Technology, The University of Oklahoma, Norman, Oklahoma 73019, USA **

(Dated: May 26, 2026)

Measurements can drive quantum many-body systems into nontrivial steady states and induce interesting dynamical phase transitions, rendering measurement-only quantum circuits a useful platform for exploring quantum many-body phases beyond those of equilibrium Hamiltonian systems. Here we study a class of long-range measurement-only quantum circuits with competing two-qubit and three-qubit measurements. We demonstrate that these circuits exhibit rich steady-state structure and uncover a strong influence of the measurement range on the resulting phases. In particular, states with symmetry-protected topological (SPT) order can emerge with sufficiently short-range measurements beyond the nearest-neighbor limit. These states feature robust topological edge modes, which can also be detected from circuit dynamics. With longer-range measurements, an extended parameter regime emerges in which conventional order parameters are suppressed while spatial correlations remain nontrivial. Moreover, we show that in this circuit model sufficiently long-range measurements can produce significant entanglement with scaling beyond an area law despite the absence of any unitary evolution.

I. INTRODUCTION

Measurements provide a powerful tool for shaping quantum many-body states beyond their conventional role as readout operations. Repeated measurements can alter entanglement structure, generate nontrivial steady states, and drive dynamical phase transitions. A prominent example is the measurement-induced phase transition in monitored quantum dynamics, where the steady-state entanglement changes qualitatively as the measurement rate is varied [1–9]. Recent developments in using measurements as an active element of many-body dynamics have opened a new route to studying phases and critical phenomena out of equilibrium, where the organizing principles can arise not only from Hamiltonian evolution but also from measurement backaction and measurement outcomes [10–32].

A particularly useful setting is provided by measurement-only quantum circuits, where the quantum dynamics is driven entirely by measurements rather than unitary gates. Such circuits have been shown to realize rich dynamical behavior, including entanglement phase transitions, purification transitions, and steady states with nontrivial ordering or topological character [14, 33–40]. In particular, measurement-only dynamics can support symmetry-protected topological features and symmetry-enriched critical behavior, demonstrating that measurement-generated steady states can possess structure beyond entanglement scaling alone [40–43].

Meanwhile, an important ingredient that can affect quantum many-body behavior is long-range connectivity. Long-range interactions occur naturally in a variety of quantum simulation platforms, including trapped ions, Rydberg atom arrays, dipolar atom ensembles, and

cavity-QED systems, where interactions or effective couplings can extend over many lattice spacings [44–48]. In Hamiltonian systems, such long-range coupling effects can strongly modify both equilibrium phase structure and dynamical properties, including correlation propagation and entanglement behavior, compared with short-range systems [48–57]. In monitored quantum circuits, long-range interactions have been shown to alter entanglement dynamics and measurement-induced transitions [58, 59]. More recently, long-range measurements have begun to be explored in measurement-only circuit settings, where they can produce dynamical behavior distinct from circuits with short-range measurements [60, 61]. A natural question is therefore how nonlocality entering through the spatial structure of the measurements affects many-body order when the steady state is generated by measurements rather than relying on unitary evolution.

In this work, we address this question using a class of measurement-only circuits with competing two- and three-qubit projective measurements. The circuit contains cluster measurements favoring a symmetry-protected topological (SPT) structure and Ising-type measurements whose range is tunable through a control parameter α . In the large α limit, the model reduces to a nearest-neighbor Ising-cluster measurement circuit, while finite α introduces a nonlocal structure that directly competes with the SPT-generating cluster measurements.

We characterize the steady-state phase structure as the measurement probability and measurement range vary. By examining relevant order parameters, we find that an SPT phase survives weak long-range measurement effects at strong cluster measurement rates, despite being destabilized when the Ising measurements become sufficiently long-ranged. Strong Ising measurements establish a long-range ordered regime analogous to the ferromagnetic spontaneous-symmetry-breaking (SSB) phase

* bihui.zhu@ou.edu

in equilibrium many-body systems, which we refer to as the SSB phase here. This SSB phase is enhanced as longer-range two-qubit measurements couple more distant sites, but it does not simply replace the destroyed SPT phase. Rather, at larger measurement range, another extended regime emerges in which the usual SPT and SSB order parameters are both suppressed. This new regime harbors nontrivial structure beyond a simple disordered steady state. The half-chain entanglement entropy is strongly enhanced there and shows clear growth beyond an area law with system size for sufficiently long-ranged measurements. Correlation functions further reveal competing spin-spin and string correlations, which can exhibit nearly algebraic decay and symmetry-enriched critical-like behavior in part of this regime.

Purification dynamics and edge responses further reveal the topological character of the SPT regime. In the parameter regime corresponding to the SPT phase, purification dynamics shows a larger nonvanishing residual entanglement entropy at late times than in the SSB regime, indicating the existence of topological edge states. Additionally, the edge-qubit response to boundary perturbations remains robust for large α and strong cluster measurements.

The rest of the paper is organized as follows. In Sec. II, we introduce the long-range measurement-only circuit model considered in this work. In Sec. III A, we characterize the steady-state phase structure using the corresponding order parameters, purification dynamics, and edge responses. In Sec. III B, we analyze the half-chain entanglement entropy and its scaling with system size. In Sec. IV, we further study spin-spin and string correlation functions. Finally, in Sec. V, we summarize our results and discuss possible future directions.

II. CIRCUIT MODEL

We study a family of one-dimensional measurement-only circuits as illustrated schematically in Fig. 1. The circuit architecture consists of a set of measurements $\{Z_{i-1}X_iZ_{i+1}, Z_iZ_{i+1}\}$, which preserve a \mathbb{Z}_2 symmetry given by the global term $\prod_{i=1}^L X_i$. At each discrete time step, a measurement is applied randomly: with probability p_{ZZ} a two-qubit measurement Z_iZ_j is applied on a pair of qubits (i, j) , drawn from a power-law distribution over the set of all distinct pairs \mathcal{P} ,

$$P(i, j) = \mathcal{N} \frac{1}{|i - j|^\alpha}, \quad (1)$$

where $\mathcal{N} = (\sum_{(m,n) \in \mathcal{P}} |m - n|^{-\alpha})^{-1}$ is the normalization factor, with open boundary conditions. With probability $1 - p_{ZZ}$, the three-site measurement $Z_{i-1}X_iZ_{i+1}$ is applied, with the center i chosen uniformly from the L qubits on the one-dimensional chain. As such, the two-qubit measurements allow qubits separated by long distances to be coupled together.

Such a circuit model contains no unitary gates; instead, the two types of projective measurements do not commute with each other and drive the quantum dynamics toward a steady state. Since all measurements are Pauli measurements, the circuit consists solely of Clifford operations, which map Pauli strings to Pauli strings. This structure allows the dynamics to be efficiently simulated using the stabilizer formalism based on the Gottesman-Knill theorem [62–64]. In this formalism, the many-body state is represented compactly by a set of stabilizer generators, rather than by the full wavefunction in the exponentially large Hilbert space [4, 8, 65]. In this work, we adopt such an approach to numerically evolve the quantum circuit and study the steady-state structure generated by the competing measurements.

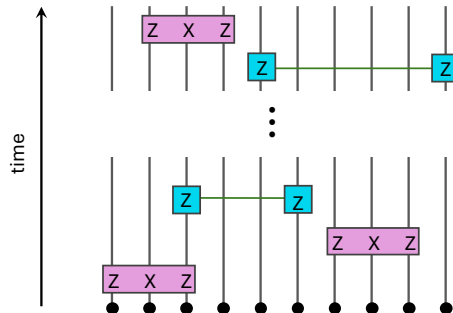


FIG. 1. Schematic of the long-range measurement-only quantum circuit. The circuit dynamics is driven by two types of measurements, the three-qubit cluster measurements and the ZZ measurements on two qubits.

III. PHASE STRUCTURE AT THE STEADY STATE

A. SPT and symmetry-breaking phases

The Hamiltonian counterpart of this circuit model with nearest-neighbor interactions features an SSB phase and an SPT phase in the ground state, when the corresponding two-body Ising term and three-body cluster term dominate, respectively [66, 67]. In the measurement-only circuit model, starting from the initial state $|\psi_0\rangle = \prod_{i=1}^L |+\rangle_i$, with $|+\rangle$ the positive eigenstate of the Pauli X operator, the noncommuting random measurements generate dynamical evolution of the quantum state. In the steady state, the system exhibits distinct orders depending on the competition between the two types of measurements. In particular, a circuit with only the three-qubit $Z_{i-1}X_iZ_{i+1}$ measurements projects the system into the cluster state with SPT order [14, 68]; with only the two-qubit measurements, a long-range order emerges in the steady state analogous to the SSB phase in the ground state scenario [69]. In both cases, the entanglement entropy obeys an area law with the system size. These different steady-state phases can be characterized through

the following order parameters:

$$O_{\text{SSB}} = |\langle Z_a Z_b \rangle|, \quad (2)$$

$$O_{\text{SPT}} = |\langle Z_{a-1} Y_a \prod_{a < k < b} X_k Y_b Z_{b+1} \rangle|, \quad (3)$$

in which we fix a (b) to be at a distance $L/4$ from the left (right) edge of the qubit chain to reduce the boundary effect.

In the quantum circuit setting, the state of the system evolves along different trajectories under random measurements. In the context of measurement-induced phase transitions, the dynamical phase transition is generally not captured by linear observables evaluated on the ensemble-averaged density matrix of the system, but instead depends on trajectory-resolved properties [2, 4]. Here, a direct average of the signed expectation values of these correlation operators over trajectories can vanish due to cancellations between symmetry-related trajectories. To detect the phase transitions, these order parameters are therefore computed by taking the absolute value of the trajectory-resolved expectation value before averaging over trajectories [70]. In this work, for all results shown we average over at least 10^4 trajectories for each circuit parameter setting considered, evolve circuits for at least $4L^2$ time steps to establish the steady state, and focus on system size $L = 128$ unless otherwise specified.

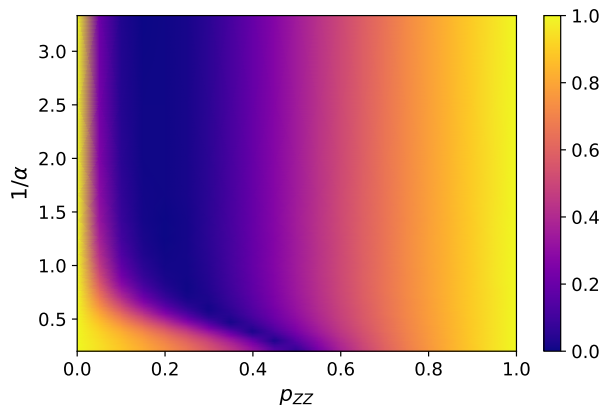


FIG. 2. Steady-state phase diagram of the long-range measurement-only circuit, characterized by $\max(O_{\text{SSB}}, O_{\text{SPT}})$ (color bar).

With nearest-neighbor-only measurements, the phase transition between the SPT and SSB phases is expected to occur at $p_{ZZ} = p_{ZXZ} = 0.5$ [40]. The presence of long-range coupling affects the competition between these two types of measurements that drive the circuit dynamics and modifies the steady-state phase structure. In Fig. 2, we evolve the circuit under the competing measurements and plot the larger of the two order parameters, namely $\max(O_{\text{SSB}}, O_{\text{SPT}})$, computed in the steady state and across different measurement probabilities p_{ZZ} and the parameter controlling the range of measurements,

$1/\alpha$. For $1/\alpha \ll 1$, the behavior of the system approximates the case of nearest-neighbor measurements and undergoes a phase transition when $p_{ZZ} \approx p_{ZXZ}$. As $1/\alpha$ increases, far apart qubits can be effectively coupled, which enhances the collective order built from the two-qubit ZZ measurements, and the SSB phase region extends to smaller p_{ZZ} . Nevertheless, the SPT phase appears to persist at small $1/\alpha$ and sufficiently low p_{ZZ} , before longer-range two-qubit measurements eventually destabilize the SPT order. In Appendix A, we also examine the corresponding generalized topological entropy, which serves as an order parameter for the SPT phase in short-range systems and indicates behavior consistent with these findings [14, 71]. Further finite-size scaling analysis (see Appendix B) suggests that the SPT phase is destroyed for long-range measurements with $\alpha < 2$. Meanwhile, longer-range measurements do not continue to establish the SSB order at smaller p_{ZZ} , which is interrupted in the presence of frequent cluster measurements; instead, an extended region emerges below moderately large p_{ZZ} where both O_{SSB} and O_{SPT} appear vanishingly small.

To analyze the structure of the steady state generated by the circuit dynamics, we also examine the purification dynamics in this circuit model, starting from a maximally mixed initial state $\rho = \mathbb{I}/2^L$ [8]. In Fig. 3, the full system entanglement entropy $S(t)$ is shown for two representative measurement ranges, with $\alpha = 1$ and $\alpha = 3$ and for different measurement probabilities p_{ZZ} . With $p_{ZZ} = 0$, the steady state reaches the cluster state with SPT order, and the residual entropy $S(t) = 2$ at late times indicates two bits of unpurified information, reflecting the existence of four-fold degenerate topological edge states on the open chain [68, 72]. For $\alpha = 1$, with both small and large $p_{ZZ} > 0$, the late-time residual entropy is reduced to $S(t) = 1$, indicating that the four-fold SPT edge degeneracy is no longer present, with the remaining residual entropy arising from a different, symmetry-breaking origin. In contrast, for $\alpha = 3$, the residual entropy remains $S(t) = 2$ at late times for small p_{ZZ} within the time window considered, consistent with the presence of edge states associated with the SPT order.

To probe this edge structure more directly at the steady state, we implement an edge-probe protocol. In equilibrium Hamiltonian systems, an SPT-ordered phase on an open chain supports boundary degrees of freedom associated with the nontrivial bulk topology [73]. A small boundary field can polarize these edge modes and induce a strong edge response, even when the field remains much smaller than the bulk gap. For the cluster SPT, the open boundary supports effective edge spin-1/2 degrees of freedom, which can be probed through their response to appropriate boundary operators [68]. In contrast, in a topologically trivial phase, where no protected boundary degree of freedom is present, the response is expected to scale approximately linearly with the applied field in the weak-field regime, exhibiting behavior distinct from the SPT case.

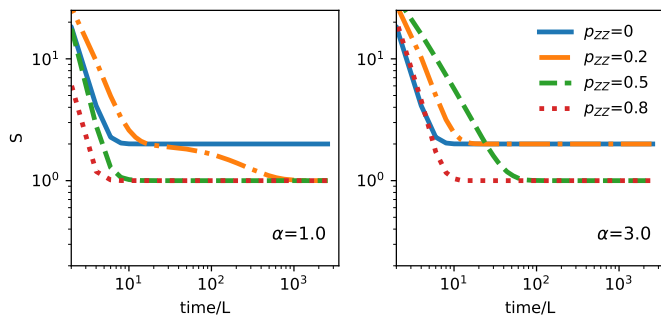


FIG. 3. Purification dynamics. The time-evolution of the full-system entanglement entropy S is plotted for two different ranges of the ZZ measurements, $\alpha = 1$ (left) and $\alpha = 3$ (right). Different lines represent the dynamics obtained at various different measurement probabilities p_{ZZ} .

In our circuit setting, we implement the analogous probe dynamically by adding measurements X_1Z_2 and $Z_{L-1}X_L$ on the left and right boundary qubits with probability p_b [74–76]. We then characterize the resulting edge polarization at the steady state by

$$M_b = \frac{|\langle X_1Z_2 \rangle| + |\langle Z_{L-1}X_L \rangle|}{2}. \quad (4)$$

In Fig. 4, we show the edge response as a function of the boundary measurement probability p_b in different parameter regimes. For large p_{ZZ} , M_b decreases rapidly as p_b is reduced, consistent with the system being outside the nontrivial SPT phase when the two-qubit measurements dominate. In contrast, at $p_{ZZ} = 0$, M_b stays finite at weak boundary measurement strengths, as expected for the cluster SPT state. For $\alpha = 3$ with sufficiently small p_{ZZ} , M_b remains robust at weak p_b , providing further evidence for a nontrivial SPT steady-state regime.

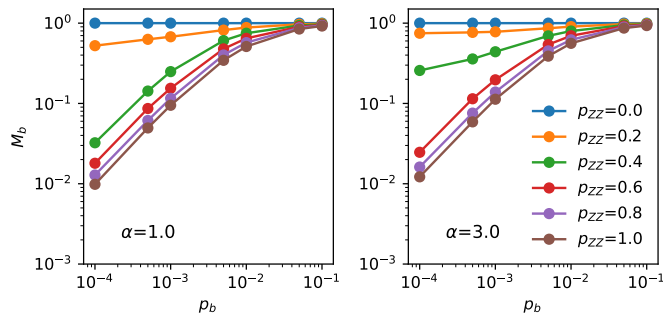


FIG. 4. Edge responses at the steady state when a boundary measurement perturbation is applied with probability p_b , in a circuit with the two-qubit measurements of $\alpha = 1$ (left) and $\alpha = 3$ (right). Different colors represent the results obtained at different two-qubit measurement probabilities, ranging from $p_{ZZ} = 0$ to $p_{ZZ} = 1$.

B. Beyond area-law entanglement

In this section, we examine the entanglement generated in the steady state by the circuit dynamics starting from the initial product state. Specifically, we compute the half-chain von Neumann entanglement entropy $S_{\text{half}} = -\text{Tr}[\rho_{\text{half}} \log \rho_{\text{half}}]$, where ρ_{half} is the reduced density matrix of the half-chain subsystem, across different measurement probabilities p_{ZZ} and measurement ranges controlled by α . For the stabilizer circuits considered in this work, this entropy is identical to the Rényi entropies as stabilizer states have flat entanglement spectra [77]. As shown in Fig. 5, for short-range measurements, $1/\alpha \ll 1$, and away from the phase boundary, the generated entanglement remains relatively small, while it becomes strongly enhanced in the intermediate parameter regime and with small α . This enhancement is associated with the same part of the phase diagram in which Fig. 2 indicates neither SPT nor SSB order, suggesting the emergence of a highly entangled steady-state regime.

To further check the entanglement behavior in the intermediate parameter regime, we compute the steady-state S_{half} as a function of system size L at fixed p_{ZZ} and for different measurement ranges controlled by α . For comparing the entanglement scaling with L across different α 's, we normalize the steady-state S_{half} at each parameter α by its value obtained for the smallest system size L considered in Fig. 6. As this figure shows, the measurement range induces qualitatively different behaviors in steady-state entanglement scaling. For long-range measurements with $\alpha \lesssim 2$ considered here, a clear growth in the entanglement beyond an area law is found. In particular, at $\alpha = 2$, the half-chain entanglement entropy exhibits critical-like logarithmic scaling. As shown for $\alpha \geq 3$, the entanglement growth remains close to an area law. These results are consistent with the observation of a strongly increased entanglement entropy in the intermediate region in Fig. 5. We note that in systems with power-law interacting Hamiltonians and long-range unitary gates, similar strong modifications of the entanglement properties have been suggested [51, 52, 58, 78, 79], while here the entanglement arises solely from projective measurements rather than unitary time evolution.

IV. CORRELATIONS AND SYMMETRY-ENRICHED BEHAVIOR

In this section, we take a closer look at the intermediate regime revealed in Figs. 2 and 5, where both the SSB and the SPT order parameters, O_{SSB} and O_{SPT} , appear suppressed. To this end, we compute the connected spin-spin correlation function $C_{ZZ}(r)$ and the nonlocal string correlation function $C_{\text{SPT}}(r)$ at the steady state

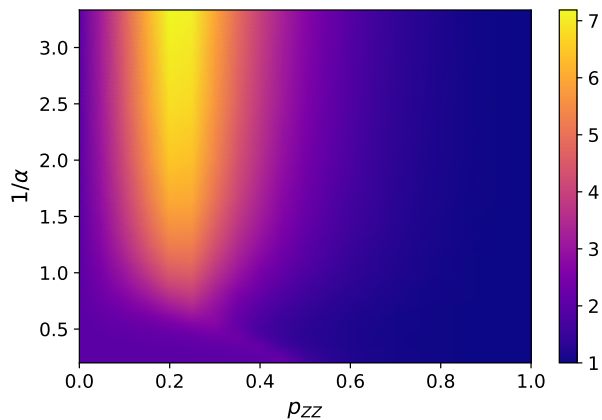


FIG. 5. Half-chain entanglement entropy at the steady state. The color bar indicates the value of S_{half} .

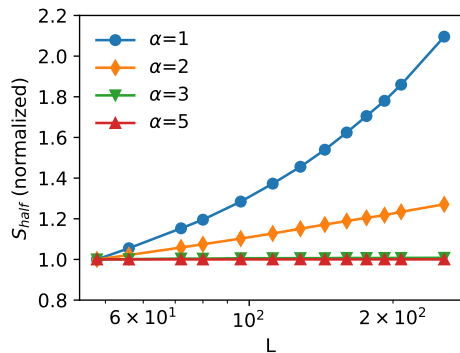


FIG. 6. Entanglement entropy scaling with system sizes. The half-chain entanglement entropy at the steady-state is computed at fixed $p_{ZZ} = 0.3$ for various α 's. For each α , $S_{\text{half}}(L)$ normalized by the corresponding value at the smallest L is plotted. Here $L = 48$ is used.

as a function of the site distance r , defined as

$$C_{ZZ}(r) = |\langle Z_i Z_{i+r} \rangle - \langle Z_i \rangle \langle Z_{i+r} \rangle|, \quad (5)$$

$$C_{\text{SPT}}(r = |j - i|) = |\langle Z_{i-1} Y_i \prod_{k=i+1}^{j-1} X_k Y_j Z_{j+1} \rangle|. \quad (6)$$

For a range of moderate α and p_{ZZ} values, we find both the spin correlations $C_{ZZ}(r)$ and string correlations $C_{\text{SPT}}(r)$ display approximately power-law decay with distance r , reminiscent of the behavior of critical states in short-range interacting systems. Interestingly, in part of this intermediate region, $C_{\text{SPT}}(r)$ decays more slowly than $C_{ZZ}(r)$, suggesting a symmetry-enriched steady-state regime of this circuit [80, 81]. Fig. 7 shows the decay of correlations at representative parameter points, with power-law fits of the form $C(r) = Ar^{-\Delta}$ for each case also plotted for reference. With short-range measurements and intermediate $p_{ZZ} = 0.35$ (orange), the string correlations appear constant across large distances, while the connected spin-spin correlations $C_{ZZ}(r)$ decrease rapidly

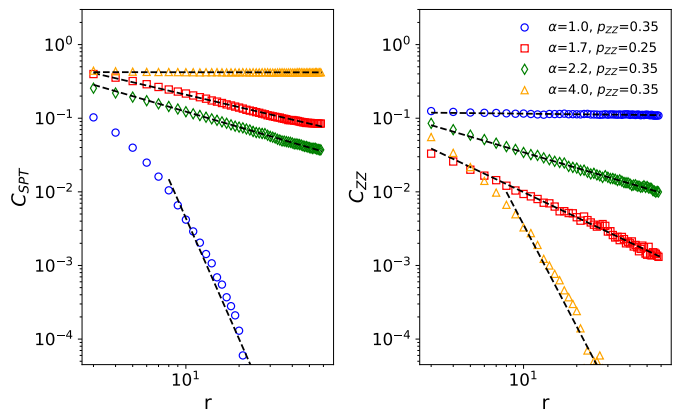


FIG. 7. Decay of string correlations C_{SPT} (left) and connected spin-spin correlations C_{ZZ} (right), plotted in double logarithmic scale.

with distance, consistent with the system being in the SPT phase as discussed in Sec. III A. At intermediate α and p_{ZZ} considered here, both correlations exhibit algebraic decay over a broad range of distances, illustrating a nontrivial interplay between long-range interactions and topology. In particular, for the results colored in red, $\Delta_{\text{SPT}} \approx 0.56$ and $\Delta_{ZZ} \approx 1.13$ respectively, indicating that the string correlations dominate over the two-body spin-spin correlations at large distances. This suggests a scenario where the SPT character remains visible in the long-distance correlations despite the apparent suppression of the string order parameter. The results colored in green demonstrate the scenario in which the two types of correlations exhibit comparable long-distance scaling, with $\Delta_{\text{SPT}} \approx 0.7$ and $\Delta_{ZZ} \approx 0.7$. Related behaviors in ground-state phases of Hamiltonian systems were also found in a recent study, where the power-law interactions introduce anomalous effects absent in short-range interacting systems [82]. For the small α (blue) shown in the figure, the string correlation decays exponentially, suggesting the absence of the SPT order, while the connected spin-spin correlation displays only a very weak decay over the distances accessed, with $\Delta_{ZZ} \approx 0.03$, suggesting a quasi-long-range order resulting from sufficiently long-range measurements.

V. SUMMARY AND OUTLOOK

In this work, we studied a class of long-range measurement-only circuits constructed from competing two-qubit Ising measurements and three-qubit cluster measurements. The Ising measurements involve two qubits separated at distances beyond nearest neighbors, with the effective range tunable through α . Using order parameters derived from the nonlocal string correlations and ferromagnetic correlations used to detect SPT and SSB orders in equilibrium phases and adapted to the nonequilibrium circuit settings, we showed that

the steady states in these circuits can display distinct measurement-induced orders depending on the strength of the measurements and the measurement range. In particular, we demonstrated the persistence of SPT order beyond the nearest-neighbor limit, whose presence also manifests through a larger residue entropy in the purification dynamics and robust edge responses. We also found that long-range measurements introduce an extended region in parameter space which does not feature pronounced order parameters while exhibiting rich structure through spatial string and connected spin-spin correlations. We further analyzed the quantum entanglement generated at the steady states, and the modification from long-range effects is found to be strongest in the intermediate parameter regime, with clear beyond-area-law entanglement at small α .

Our results illustrate that spatially structured measurements may provide a useful tool for engineering quantum many-body states with nontrivial orders and for studying nonequilibrium phases and critical-like phenomena. The effect of long-range measurements has a significant impact on phase organization beyond simply destroying one phase while stabilizing the other. An interesting direction for future work concerns a more detailed analysis of the phase boundaries and universality classes of relevant phase transitions, especially of the properties in the intermediate α regime. Furthermore, the circuit setup considered here realizes a scenario that is related to a ferromagnetic cluster-Ising Hamiltonian counterpart, where long-range Ising couplings are expected to have a strong effect. Another possible direction would be to explore setups where the measurement protocols impose antiferromagnetic parity constraints, for example through suitable postselection of measurement outcomes. In long-range settings, such constraints can become mutually frustrated, potentially leading to a different interplay between long-range effects and topological structure and giving rise to new many-body behaviors. The family of circuits considered here provides one example of long-range circuits with nontrivially ordered phases, and it would be interesting to extend the study to other types of phases, including those that may emerge in higher-dimensional circuits.

ACKNOWLEDGMENTS

We thank the Kavli Institute for Theoretical Physics (KITP) for hospitality while part of this work was completed. We acknowledge support from the National Science Foundation through grants LEAPS-MPS 2317030 and CAREER Award 2443398. This work used Anvil at Purdue University through allocation PHY260116 from the Advanced Cyberinfrastructure Coordination Ecosystem: Services & Support (ACCESS) program, which is supported by U.S. National Science Foundation grants #2138259, #2138286, #2138307, #2137603, and #2138296 [83].

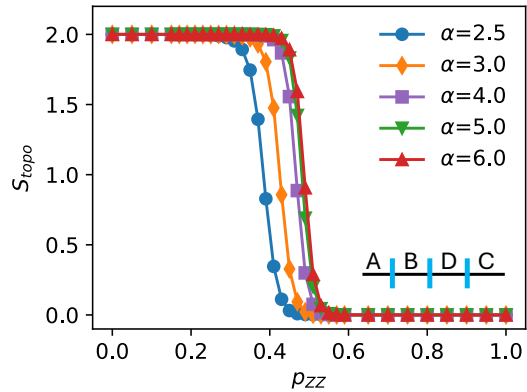


FIG. 8. Generalized topological entanglement entropy S_{topo} . The inset depicts the geometry used in the definition of S_{topo} , where the chain is divided into four equal regions.

Appendix A: Generalized topological entanglement entropy

In this section, we investigate additional probes for the SPT order. To this end, we consider a generalized topological entanglement entropy, which has been used as an order parameter for the SPT phase in gapped ground states and in nearest-neighbor coupled circuits [14, 41, 71, 84]. For a one dimensional chain as in our circuit model, partitioning the system into four regions as depicted in Fig. 8, the generalized topological entanglement entropy S_{topo} is defined as:

$$S_{\text{topo}} = S_{AB} + S_{BC} - S_B - S_{ABC}, \quad (\text{A1})$$

where S_{AB} denotes the entanglement entropy for the subsystem AB . For gapped Hamiltonian systems, S_{topo} is quantized in the thermodynamic limit and its nonzero value is a signature of SPT order. For the cluster state in particular, $S_{\text{topo}} = 2$. In Fig. 8, we compute S_{topo} as the two-qubit measurement probability varies for several different α 's. As sufficiently long-range couplings can contribute additional nonlocal entanglement, we restrict here to moderately large α . As Fig. 8 indicates, for small p_{ZZ} , S_{topo} stays at 2, and quickly drops to 0 above a certain threshold of p_{ZZ} , reflecting a transition from a nontrivial SPT order to a trivial one. For large α , this threshold is around 0.5, and is nearly identical for $\alpha = 5$ and 6, suggesting behavior close to the nearest-neighbor cases. Similar behaviors are observed for smaller $\alpha > 2$, while the threshold is shifted toward smaller p_{ZZ} as α is reduced, consistent with the findings revealed from O_{SPT} and O_{SSB} in the main text.

Appendix B: Additional results for different system sizes

In Sec. III, we presented the results obtained from numerically simulating circuits of size $L = 128$. Here, we

extend the analysis of the order parameters for a range of different system sizes to account for finite-size effects. In each panel of Fig. 9 and Fig. 10, we compute O_{SPT} and O_{SSB} , respectively, for representative α values, from very long-range to approximately short-range measurement regimes, and each panel corresponds to a fixed two-qubit measurement probability, ranging from small

to large p_{ZZ} (left to right). As these figures show, for moderately large α , the SPT order parameter remains finite within the accessible system sizes when p_{ZZ} is sufficiently small, while for very small α such as $\alpha = 1$, the SSB order parameter remains suppressed at relatively low p_{ZZ} . These results provide further evidence for the phase structure discussed in the main text.

-
- [1] Y. Li, X. Chen, and M. P. A. Fisher, Quantum Zeno effect and the many-body entanglement transition, *Physical Review B* **98**, 205136 (2018).
- [2] B. Skinner, J. Ruhman, and A. Nahum, Measurement-induced phase transitions in the dynamics of entanglement, *Phys. Rev. X* **9**, 031009 (2019).
- [3] A. Chan, R. M. Nandkishore, M. Pretko, and G. Smith, Unitary-projective entanglement dynamics, *Phys. Rev. B* **99**, 224307 (2019).
- [4] Y. Li, X. Chen, and M. P. A. Fisher, Measurement-driven entanglement transition in hybrid quantum circuits, *Phys. Rev. B* **100**, 134306 (2019).
- [5] Y. Bao, S. Choi, and E. Altman, Theory of the phase transition in random unitary circuits with measurements, *Phys. Rev. B* **101**, 104301 (2020).
- [6] C.-M. Jian, Y.-Z. You, R. Vasseur, and A. W. W. Ludwig, Measurement-induced criticality in random quantum circuits, *Phys. Rev. B* **101**, 104302 (2020).
- [7] A. Zabalo, M. J. Gullans, J. H. Wilson, S. Gopalakrishnan, D. A. Huse, and J. H. Pixley, Critical properties of the measurement-induced transition in random quantum circuits, *Phys. Rev. B* **101**, 060301(R) (2020).
- [8] M. J. Gullans and D. A. Huse, Dynamical purification phase transition induced by quantum measurements, *Phys. Rev. X* **10**, 041020 (2020).
- [9] Q. Tang and W. Zhu, Measurement-induced phase transition: A case study in the nonintegrable model by density-matrix renormalization group calculations, *Phys. Rev. Res.* **2**, 013022 (2020).
- [10] M. P. Fisher, V. Khemani, A. Nahum, and S. Vijay, Random quantum circuits, *Annual Review of Condensed Matter Physics* **14**, 335 (2023).
- [11] C. Noel, P. Niroula, D. Zhu, A. Risinger, L. Egan, D. Biswas, M. Cetina, A. V. Gorshkov, M. J. Gullans, D. A. Huse, *et al.*, Measurement-induced quantum phases realized in a trapped-ion quantum computer, *Nature Physics* **18**, 760 (2022).
- [12] A. J. Friedman, O. Hart, and R. Nandkishore, Measurement-induced phases of matter require feedback, *PRX Quantum* **4**, 040309 (2023).
- [13] M. J. Gullans and D. A. Huse, Scalable probes of measurement-induced criticality, *Phys. Rev. Lett.* **125**, 070606 (2020).
- [14] A. Lavasani, Y. Alavirad, and M. Barkeshli, Measurement-induced topological entanglement transitions in symmetric random quantum circuits, *Nature Physics* **17**, 342 (2021).
- [15] M. Szyniszewski, A. Romito, and H. Schomerus, Universality of entanglement transitions from stroboscopic to continuous measurements, *Phys. Rev. Lett.* **125**, 210602 (2020).
- [16] O. Lunt and A. Pal, Measurement-induced entanglement transitions in many-body localized systems, *Phys. Rev. Res.* **2**, 043072 (2020).
- [17] S. Choi, Y. Bao, X.-L. Qi, and E. Altman, Quantum error correction in scrambling dynamics and measurement-induced phase transition, *Phys. Rev. Lett.* **125**, 030505 (2020).
- [18] R. Fan, S. Vijay, A. Vishwanath, and Y.-Z. You, Self-organized error correction in random unitary circuits with measurement, *Phys. Rev. B* **103**, 174309 (2021).
- [19] Y. Li and M. P. A. Fisher, Statistical mechanics of quantum error correcting codes, *Phys. Rev. B* **103**, 104306 (2021).
- [20] Y. Bao, S. Choi, and E. Altman, Symmetry enriched phases of quantum circuits, *Annals of Physics* **435**, 168618 (2021), special issue on Philip W. Anderson.
- [21] X. Turkeshi, A. Biella, R. Fazio, M. Dalmonte, and M. Schiró, Measurement-induced entanglement transitions in the quantum ising chain: From infinite to zero clicks, *Phys. Rev. B* **103**, 224210 (2021).
- [22] S. Sang, Y. Li, T. Zhou, X. Chen, T. H. Hsieh, and M. P. Fisher, Entanglement negativity at measurement-induced criticality, *PRX Quantum* **2**, 030313 (2021).
- [23] A. Lavasani, Y. Alavirad, and M. Barkeshli, Topological order and criticality in $(2 + 1)$ D monitored random quantum circuits, *Phys. Rev. Lett.* **127**, 235701 (2021).
- [24] A. Zabalo, M. J. Gullans, J. H. Wilson, R. Vasseur, A. W. W. Ludwig, S. Gopalakrishnan, D. A. Huse, and J. H. Pixley, Operator scaling dimensions and multifractality at measurement-induced transitions, *Phys. Rev. Lett.* **128**, 050602 (2022).
- [25] T.-C. Lu, Z. Zhang, S. Vijay, and T. H. Hsieh, Mixed-state long-range order and criticality from measurement and feedback, *PRX Quantum* **4**, 030318 (2023).
- [26] J. M. Koh, S.-N. Sun, M. Motta, and A. J. Minnich, Measurement-induced entanglement phase transition on a superconducting quantum processor with mid-circuit readout, *Nature Physics* **19**, 1314 (2023).
- [27] K. Yamamoto and R. Hamazaki, Localization properties in disordered quantum many-body dynamics under continuous measurement, *Phys. Rev. B* **107**, L220201 (2023).
- [28] A. De Luca, C. Liu, A. Nahum, and T. Zhou, Universality classes for purification in nonunitary quantum processes, *Phys. Rev. X* **15**, 041024 (2025).
- [29] Google Quantum AI and Collaborators, J. C. Hoke, M. Ippoliti, E. Rosenberg, D. Abanin, R. Acharya, T. I. Andersen, M. Ansmann, F. Arute, K. Arya, A. Asfaw, J. Atalaya, J. C. Bardin, A. Bengtsson, G. Bortoli, A. Bourassa, J. Bovaird, L. Brill, M. Broughton, B. B. Buckley, D. A. Buell, T. Burger, B. Burkett, N. Bushnell, Z. Chen, B. Chiaro, D. Chik, J. Cogan, R. Collins, P. Conner, W. Courtney, A. L. Crook, B. Curtin, A. G.

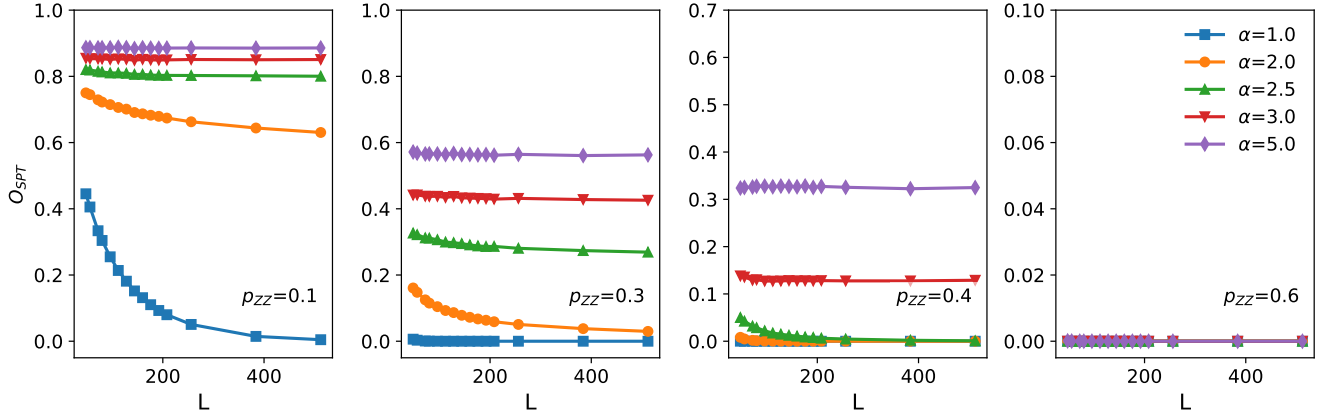


FIG. 9. String order parameter O_{SPT} at the steady state as the system size L is varied.

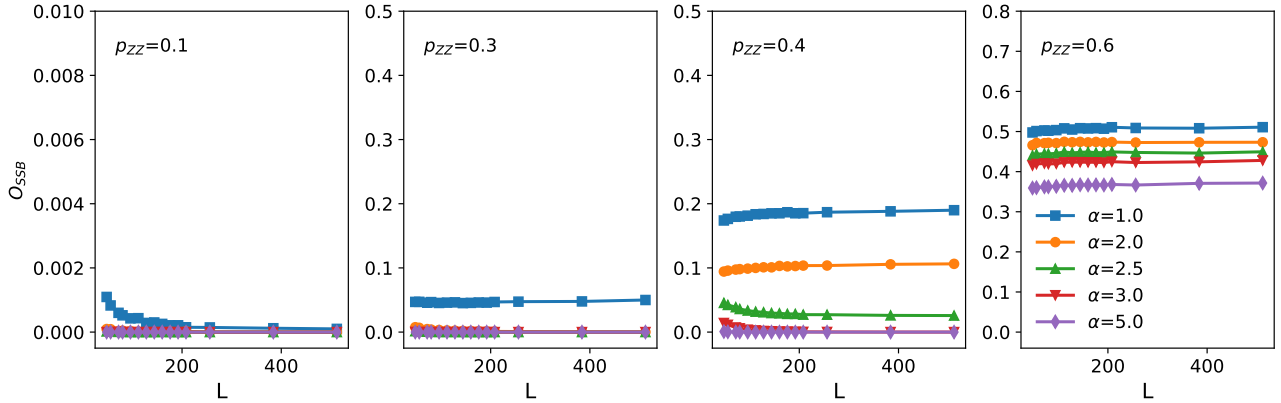


FIG. 10. SSB order parameter O_{SSB} at the steady state as the system size L is varied.

Dau, D. M. Debroy, A. Del Toro Barba, S. Demura, A. Di Paolo, I. K. Drozdov, A. Dunsworth, D. Eppens, C. Erickson, E. Farhi, R. Fatemi, V. S. Ferreira, L. F. Burgos, E. Forati, A. G. Fowler, B. Foxen, W. G. Giang, C. Gidney, D. Gilboa, M. Giustina, R. Gosula, J. A. Gross, S. Habegger, M. C. Hamilton, M. Hansen, M. P. Harrigan, S. D. Harrington, P. Heu, M. R. Hoffmann, S. Hong, T. Huang, A. Huff, W. J. Huggins, S. V. Isakov, J. Iveland, E. Jeffrey, Z. Jiang, C. Jones, P. Juhas, D. Kafri, K. Kechedzhi, T. Khattar, M. Khezri, M. Kieferová, S. Kim, A. Kitaev, P. V. Klimov, A. R. Klots, A. N. Korotkov, F. Kostritsa, J. M. Kreikebaum, D. Landhuis, P. Laptev, K.-M. Lau, L. Laws, J. Lee, K. W. Lee, Y. D. Lensky, B. J. Lester, A. T. Lill, W. Liu, A. Locharla, O. Martin, J. R. McClean, M. McEwen, K. C. Miao, A. Mieszala, S. Montazeri, A. Morvan, R. Movassagh, W. Mruzckiewicz, M. Neeley, C. Neill, A. Nersisyan, M. Newman, J. H. Ng, A. Nguyen, M. Nguyen, M. Y. Niu, T. E. O'Brien, S. Omonije, A. Opremcak, A. Petukhov, R. Potter, L. P. Pryadko, C. Quintana, C. Rocque, N. C. Rubin, N. Saei, D. Sank, K. Sankaragomathi, K. J. Satzinger, H. F. Schurkus, C. Schuster, M. J. Shearn, A. Shorter, N. Shutty, V. Shvarts, J. Skrzyny, W. C. Smith, R. Somma, G. Sterling, D. Strain, M. Szalay, A. Torres, G. Vidal, B. Vil-

alonga, C. V. Heidweiller, T. White, B. W. K. Woo, C. Xing, Z. J. Yao, P. Yeh, J. Yoo, G. Young, A. Zalcman, Y. Zhang, N. Zhu, N. Zobrist, H. Neven, R. Babbush, D. Bacon, S. Boixo, J. Hilton, E. Lucero, A. Megrant, J. Kelly, Y. Chen, V. Smelyanskiy, X. Mi, V. Khemani, and P. Roushan, Measurement-induced entanglement and teleportation on a noisy quantum processor, *Nature* **622**, 481 (2023).

- [30] M. Foss-Feig, A. Tikku, T. Lu, K. Mayer, M. Iqbal, T. Gatterman, J. Gerber, K. Gilmore, D. Gresh, A. Hankin, *et al.*, Experimental demonstration of the advantage of adaptive quantum circuits (2023), arXiv preprint arXiv:2302.03029.
- [31] E. Bäumer, V. Tripathi, D. S. Wang, P. Rall, E. H. Chen, S. Majumder, A. Seif, and Z. K. Mineev, Efficient long-range entanglement using dynamic circuits, *PRX Quantum* **5**, 030339 (2024).
- [32] Z. Xiao and K. Kawabata, Symmetry and topology of monitored quantum dynamics, *Phys. Rev. B* **113**, 134307 (2026).
- [33] M. Ippoliti, M. J. Gullans, S. Gopalakrishnan, D. A. Huse, and V. Khemani, Entanglement phase transitions in measurement-only dynamics, *Phys. Rev. X* **11**, 011030 (2021).

- [34] S. Sang and T. H. Hsieh, Measurement-protected quantum phases, *Phys. Rev. Res.* **3**, 023200 (2021).
- [35] N. Lang and H. P. Büchler, Entanglement transition in the projective transverse field Ising model, *Physical Review B* **102**, 094204 (2020).
- [36] A. Lavasani, Z.-X. Luo, and S. Vijay, Monitored quantum dynamics and the Kitaev spin liquid, *Phys. Rev. B* **108**, 115135 (2023).
- [37] K. Klocke and M. Buchhold, Majorana loop models for measurement-only quantum circuits, *Phys. Rev. X* **13**, 041028 (2023).
- [38] T. Orito, Y. Kuno, and I. Ichinose, Measurement-only dynamical phase transition of topological and boundary order in toric code and gauge higgs models, *Phys. Rev. B* **109**, 224306 (2024).
- [39] Y. Kuno and I. Ichinose, Production of lattice gauge Higgs topological states in a measurement-only quantum circuit, *Physical Review B* **107**, 224305 (2023).
- [40] X.-J. Yu, S. Yang, S. Liu, H.-Q. Lin, and S.-K. Jian, Gapless Symmetry-Protected Topological States in Measurement-Only Circuits (2025), arXiv:2501.03851 [cond-mat].
- [41] K. Klocke and M. Buchhold, Topological order and entanglement dynamics in the measurement-only XZZX quantum code, *Physical Review B* **106**, 104307 (2022).
- [42] Y. Kuno and I. Ichinose, Emergence symmetry protected topological phase in spatially tuned measurement-only circuit, arXiv preprint arXiv:2212.13142 (2022).
- [43] H. Yu and J. Hu, Measurement-driven transitions between area law phases, *Physica Scripta* **100**, 065950 (2025).
- [44] C. Monroe, W. C. Campbell, L.-M. Duan, Z.-X. Gong, A. V. Gorshkov, P. W. Hess, R. Islam, K. Kim, N. M. Linke, G. Pagano, P. Richerme, C. Senko, and N. Y. Yao, Programmable quantum simulations of spin systems with trapped ions, *Rev. Mod. Phys.* **93**, 025001 (2021).
- [45] A. Browaeys and T. Lahaye, Many-body physics with individually controlled Rydberg atoms, *Nature Physics* **16**, 132 (2020).
- [46] L. Chomaz, I. Ferrier-Barbut, F. Ferlaino, B. Laburthe-Tolra, B. L. Lev, and T. Pfau, Dipolar physics: a review of experiments with magnetic quantum gases, *Reports on Progress in Physics* **86**, 026401 (2023).
- [47] H. Ritsch, P. Domokos, F. Brennecke, and T. Esslinger, Cold atoms in cavity-generated dynamical optical potentials, *Rev. Mod. Phys.* **85**, 553 (2013).
- [48] N. Defenu, T. Donner, T. Macrì, G. Pagano, S. Ruffo, and A. Trombettoni, Long-range interacting quantum systems, *Rev. Mod. Phys.* **95**, 035002 (2023).
- [49] N. Defenu, A. Leroze, and S. Pappalardi, Out-of-equilibrium dynamics of quantum many-body systems with long-range interactions, *Physics Reports* **1074**, 1 (2024).
- [50] S. Maity, U. Bhattacharya, and A. Dutta, One-dimensional quantum many body systems with long-range interactions, *Journal of Physics A: Mathematical and Theoretical* **53**, 013001 (2020).
- [51] T. Koffel, M. Lewenstein, and L. Tagliacozzo, Entanglement entropy for the long-range ising chain in a transverse field, *Phys. Rev. Lett.* **109**, 267203 (2012).
- [52] D. Vodola, L. Lepori, E. Ercolessi, A. V. Gorshkov, and G. Pupillo, Kitaev chains with long-range pairing, *Phys. Rev. Lett.* **113**, 156402 (2014).
- [53] D. Vodola, L. Lepori, E. Ercolessi, and G. Pupillo, Long-range Ising and Kitaev models: phases, correlations and edge modes, *New Journal of Physics* **18**, 015001 (2016).
- [54] J. Schachenmayer, B. P. Lanyon, C. F. Roos, and A. J. Daley, Entanglement growth in quench dynamics with variable range interactions, *Phys. Rev. X* **3**, 031015 (2013).
- [55] Z.-X. Gong, M. F. Maghrebi, A. Hu, M. Foss-Feig, P. Richerme, C. Monroe, and A. V. Gorshkov, Kaleidoscope of quantum phases in a long-range interacting spin-1 chain, *Phys. Rev. B* **93**, 205115 (2016).
- [56] P. Richerme, Z.-X. Gong, A. Lee, C. Senko, J. Smith, M. Foss-Feig, S. Michalakis, A. V. Gorshkov, and C. Monroe, Non-local propagation of correlations in quantum systems with long-range interactions, *Nature* **511**, 198 (2014).
- [57] P. Hauke and L. Tagliacozzo, Spread of correlations in long-range interacting quantum systems, *Phys. Rev. Lett.* **111**, 207202 (2013).
- [58] M. Block, Y. Bao, S. Choi, E. Altman, and N. Y. Yao, Measurement-induced transition in long-range interacting quantum circuits, *Phys. Rev. Lett.* **128**, 010604 (2022).
- [59] S. Sharma, X. Turkeshi, R. Fazio, and M. Dalmonte, Measurement-induced criticality in extended and long-range unitary circuits, *SciPost Physics Core* **5**, 023 (2022).
- [60] Y. Kuno, T. Orito, and I. Ichinose, Phase transition and evidence of fast-scrambling phase in measurement-only quantum circuits, *Phys. Rev. B* **108**, 094104 (2023).
- [61] A. M. Gomez, F. Abney-McPeck, H.-Y. Hu, S. F. Yelin, and C. B. Dağ, Entanglement and information scrambling in long-range measurement-only circuits, arXiv preprint arXiv:2604.22022 (2026).
- [62] D. Gottesman, Class of quantum error-correcting codes saturating the quantum Hamming bound, *Physical Review A* **54**, 1862 (1996).
- [63] D. Gottesman, The Heisenberg Representation of Quantum Computers (1998), arXiv:quant-ph/9807006.
- [64] S. Aaronson and D. Gottesman, Improved simulation of stabilizer circuits, *Physical Review A* **70**, 052328 (2004).
- [65] B. Shi, X. Dai, and Y.-M. Lu, Entanglement negativity at the critical point of measurement-driven transition, arXiv preprint arXiv:2012.00040 (2020).
- [66] S. M. Giampaolo and B. C. Hiesmayr, Topological and nematic ordered phases in many-body cluster-Ising models, *Phys. Rev. A* **92**, 012306 (2015).
- [67] P. Smacchia, L. Amico, P. Facchi, R. Fazio, G. Florio, S. Pascazio, and V. Vedral, Statistical mechanics of the cluster Ising model, *Phys. Rev. A* **84**, 022304 (2011).
- [68] W. Son, L. Amico, and V. Vedral, Topological order in 1d cluster state protected by symmetry, *Quantum Information Processing* **11**, 1961 (2012).
- [69] S. Sang and T. H. Hsieh, Measurement-protected quantum phases, *Physical Review Research* **3**, 023200 (2021).
- [70] R. Morral-Yepes, F. Pollmann, and I. Lovas, Detecting and stabilizing measurement-induced symmetry-protected topological phases in generalized cluster models, *Physical Review B* **108**, 224304 (2023).
- [71] B. Zeng and D. L. Zhou, Topological and error-correcting properties for symmetry-protected topological order, *Europhysics Letters* **113**, 56001 (2016).
- [72] J. Cui, L. Amico, H. Fan, M. Gu, A. Hamma, and V. Vedral, Local characterization of one-dimensional topolog-

- ically ordered states, *Physical Review B* **88**, 125117 (2013).
- [73] F. Pollmann, E. Berg, A. M. Turner, and M. Oshikawa, Symmetry protection of topological phases in one-dimensional quantum spin systems, *Phys. Rev. B* **85**, 075125 (2012).
- [74] D. Paszko, D. C. Rose, M. H. Szymańska, and A. Pal, Edge modes and symmetry-protected topological states in open quantum systems, *PRX Quantum* **5**, 030304 (2024).
- [75] J. H. Han, E. Lake, H. T. Lam, R. Verresen, and Y. You, Topological quantum chains protected by dipolar and other modulated symmetries, *Phys. Rev. B* **109**, 125121 (2024).
- [76] J. Preskill, Ph219/CS219 Quantum Computation 2017, https://www.preskill.caltech.edu/ph219/ph219_2017.html (2017).
- [77] D. Fattal, T. S. Cubitt, Y. Yamamoto, S. Bravyi, and I. L. Chuang, Entanglement in the stabilizer formalism, arXiv preprint quant-ph/0406168 (2004).
- [78] T. Minato, K. Sugimoto, T. Kuwahara, and K. Saito, Fate of measurement-induced phase transition in long-range interactions, *Phys. Rev. Lett.* **128**, 010603 (2022).
- [79] Z.-X. Gong, M. Foss-Feig, F. G. S. L. Brandão, and A. V. Gorshkov, Entanglement area laws for long-range interacting systems, *Phys. Rev. Lett.* **119**, 050501 (2017).
- [80] T. Scaffidi, D. E. Parker, and R. Vasseur, Gapless Symmetry-Protected Topological Order, *Physical Review X* **7**, 041048 (2017).
- [81] R. Verresen, R. Thorngren, N. G. Jones, and F. Pollmann, Gapless Topological Phases and Symmetry-Enriched Quantum Criticality, *Physical Review X* **11**, 041059 (2021).
- [82] S. Yang, H.-Q. Lin, and X.-J. Yu, Gapless topological behaviors in a long-range quantum spin chain, *Communications Physics* **8**, 27 (2025).
- [83] T. J. Boerner, S. Deems, T. R. Furlani, S. L. Knuth, and J. Towns, ACCESS: Advancing innovation: NSF's advanced cyberinfrastructure coordination ecosystem: Services & support, in *Practice and Experience in Advanced Research Computing* (Association for Computing Machinery, New York, NY, USA, 2023) pp. 173–176.
- [84] I. Marvian, Symmetry-protected topological entanglement, *Phys. Rev. B* **95**, 045111 (2017).